



## Discovery and SAR of hydantoin TACE inhibitors

Wensheng Yu<sup>a,\*</sup>, Zhuyan Guo<sup>a,\*</sup>, Peter Orth<sup>a</sup>, Vincent Madison<sup>a</sup>, Lei Chen<sup>a</sup>, Chaoyang Dai<sup>b</sup>, Robert J. Feltz<sup>a</sup>, Vinay M. Girijavallabhan<sup>a</sup>, Seong Heon Kim<sup>a</sup>, Joseph A. Kozlowski<sup>a</sup>, Brian J. Lavey<sup>a</sup>, Dansu Li<sup>b</sup>, Daniel Lundell<sup>c</sup>, Xiaoda Niu<sup>c</sup>, John J. Piwinski<sup>b</sup>, Janeta Popovici-Muller<sup>b</sup>, Razia Rizvi<sup>a</sup>, Kristin E. Rosner<sup>b</sup>, Bandarpalle B. Shankar<sup>a</sup>, Neng-Yang Shih<sup>b</sup>, M. Arshad Siddiqui<sup>b</sup>, Jing Sun<sup>c</sup>, Ling Tong<sup>a</sup>, Shelby Umland<sup>c</sup>, Michael K. C. Wong<sup>a</sup>, De-yi Yang<sup>a</sup>, Guowei Zhou<sup>a</sup>

<sup>a</sup> Department of Medicinal Chemistry, Merck Research Laboratories, 2015 Galloping Hill Road, Kenilworth, NJ 07033, United States

<sup>b</sup> Department of Medicinal Chemistry, Merck Research Laboratories, 320 Bent Street, Cambridge, MA 02141, United States

<sup>c</sup> Department of Inflammation, Merck Research Laboratories, 2015 Galloping Hill Road, Kenilworth, NJ 07033, United States

### ARTICLE INFO

#### Article history:

Received 17 November 2009

Revised 28 January 2010

Accepted 29 January 2010

Available online 4 February 2010

#### Keywords:

TACE

TNF- $\alpha$  convertase

TNF- $\alpha$

TACE inhibitor

Hydantoin

Hydantoin zinc ligand

Anti-TNF

Rheumatoid arthritis

### ABSTRACT

We disclose inhibitors of TNF- $\alpha$  converting enzyme (TACE) designed around a hydantoin zinc binding moiety. Crystal structures of inhibitors bound to TACE revealed monodentate coordination of the hydantoin to the zinc. SAR, X-ray, and modeling designs are described. To our knowledge, these are the first reported X-ray structures of TACE with a hydantoin zinc ligand.

© 2010 Elsevier Ltd. All rights reserved.

Tumor necrosis factor- $\alpha$  (TNF- $\alpha$ ) is a key cytokine for innate immune response. Dysregulation and, in particular, overproduction of TNF- $\alpha$  have been implicated in a variety of autoimmune diseases such as rheumatoid arthritis, Crohn's disease, and psoriasis.<sup>1,2</sup> Current treatments include injectable anti-TNF biologics such as Enbrel<sup>®</sup> and Remicade<sup>®</sup>. However, the advantages of an orally active drug, such as patient convenience and cost reduction, make a small molecule drug highly desirable.

TNF- $\alpha$  is released from membrane-bound pro-TNF- $\alpha$  through proteolytic cleavage by the TNF- $\alpha$  converting enzyme (TACE).<sup>3</sup> There has been significant interest in the development of TACE inhibitors to modulate the level of TNF- $\alpha$  which has long been viewed as having potential to treat related inflammatory diseases.<sup>4,5</sup>

The majority of known TACE inhibitors incorporate a hydroxamic acid as the zinc chelating group.<sup>6</sup> Non-hydroxamic acid TACE inhibitors, including tartrates and hydantoins, have also been reported.<sup>7,8</sup> In the course of our program, we aimed to identify

non-hydroxamic acid TACE inhibitors. Previously we reported tartaric acid based TACE inhibitors and carboxylic acid based TACE inhibitors.<sup>8,9</sup> Herein, we report a new series of hydantoin based TACE inhibitors.

Several hydantoin containing compounds were identified as weak inhibitors, such as **1** ( $K_i = 6 \mu\text{M}$ ), from our screening collection. Soaking experiments of these hydantoin compounds into crystals of the catalytic domain of TACE (V353G)<sup>10</sup> resulted in the X-ray crystal structure of **2** shown in Figure 2. The structure revealed two molecules of **2** coexisting in the active site, but occupying different subsites (Fig. 2A). The first molecule of **2** occupies the S1' pocket whereas the second molecule of **2** binds to the S1 region. Unlike hydroxamates and tartrates which exhibit bidentate and tridentate zinc binding, respectively,<sup>8,11</sup> monodentate zinc coordination was observed with the S1 hydantoin nitrogen.<sup>7b,12</sup> The S1 hydantoin also forms multiple hydrogen bonds with the protein as indicated in Figure 2B. The amide nitrogen of the hydantoin interacts with the carbonyl oxygen of Gly349 and the oxygen of the adjacent carbonyl forms a bidentate hydrogen bond to the Glu406 side chain. In addition, the phenyl group occupies the hydrophobic non-prime site defined by the side chains of Val314,

\* Corresponding authors.

E-mail addresses: [wensheng.yu@spcorp.com](mailto:wensheng.yu@spcorp.com) (W. Yu), [zhuyan.guo@spcorp.com](mailto:zhuyan.guo@spcorp.com) (Z. Guo).

Thr347, Leu350, and Lys315 (Fig. 2A). The molecule of **2** in the S1' site revealed hydrogen bond interactions between the hydantoin carbonyl and the backbone NH of Leu348 and Gly349. The phenylacetamide group is embedded in the S1' pocket.

This crystal structure served as a starting point in our structure-based discovery of potent hydantoin TACE inhibitors. Our strategy was to design a scaffold based on the binding modes shown in Figure 2B, which would maintain the zinc binding of the hydantoin, and at the same time capture other key interactions, namely, hydrogen bonding to the backbone NH of Leu348, hydrogen bonding to Gly349, and filling the S1' pocket.

Scaffolds containing these key features were evaluated using molecular modeling techniques. The results indicated that 1*H*-indazol-3(2*H*)-one scaffold **3** (Fig. 1) would best satisfy the above criteria. Specifically, the hydantoin could maintain all the interactions near the catalytic zinc as observed in **2**. The carbonyl oxygen of the indazolone moiety would make hydrogen bonds with the backbone NH of Leu348 and Gly349; the methylene linker would ensure proper orientation of the scaffold for interactions with the S1' pocket. Furthermore, substituents on the benzene ring would reach further into the S1'/S3' pocket to establish additional interactions with the protein. The indazole NH could make a hydrogen bond with the carbonyl of Pro437. The methyl group on the hydantoin points into the non-prime side, into an area open for further substitutions.

The synthetic route to **3** is illustrated in Scheme 1 and was used for the synthesis of analogs. Compound **4** was treated with diben-

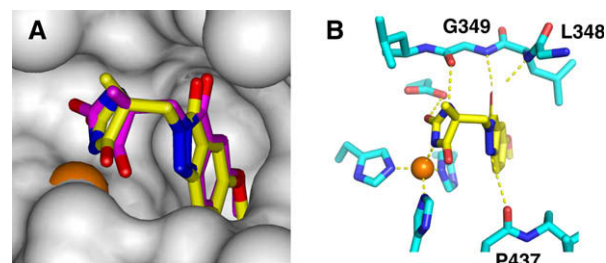
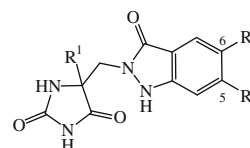


**Figure 3.** (A) Docked model of **3** (magenta) in the TACE active site (surface). The X-ray structure is shown in yellow (PDB code: 3LOV). (B) Stick representations showing the detailed interactions of **3** with the TACE active site observed in the X-ray.

**Table 1**

TACE  $K_i$  of 1*H*-indazol-3(2*H*)-ones analogs ( $\pm$ )

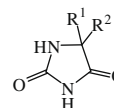


Compound	R <sup>1</sup>	R <sup>2</sup>	R <sup>3</sup>	TACE $K_i^a$ (nM)
<b>3</b>	Me	MeO	H	23
<b>8</b>	Me	H	MeO	28
<b>9</b>	Me	EtO	H	209
<b>10</b>	Me	BnO	H	391
<b>11</b>	Me	H	BnO	100
<b>12</b>	Ph	MeO	MeO	53
<b>13</b>	Ph	MeO	H	6

<sup>a</sup> The compounds were tested in a FRET assay using the catalytic domain of TACE.

**Table 2**

TACE  $K_i$  of analogs with different ring system



Compound	R <sup>1</sup>	R <sup>2</sup>	TACE $K_i^a$ (nM)
( $\pm$ )- <b>17</b>	4-F-Ph		4
( $\pm$ )- <b>18</b>	4-F-Ph		1048
( $\pm$ )- <b>19</b>	4-F-Ph		2729
( $\pm$ )- <b>20</b>	4-F-Ph		>50,000
( $\pm$ )- <b>21</b>	Me		4818
( $\pm$ )- <b>22</b>	Me		24,900
( $\pm$ )- <b>23</b>	4-F-Ph		5

<sup>a</sup> The compounds were tested in a FRET assay using the catalytic domain of TACE.

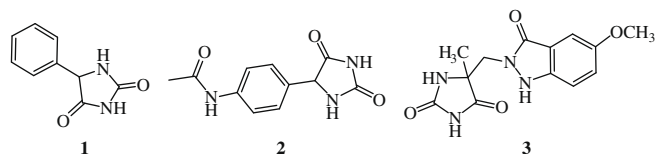


**Figure 1.** Hydantoin based TACE inhibitors

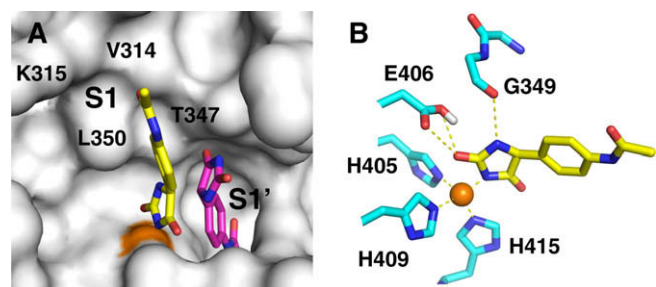
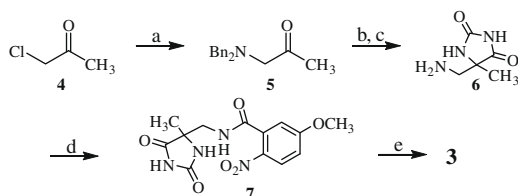


**Figure 2.** Modes of binding of compound **2** to the active site of TACE. (A) Two binding modes (cyan and yellow carbons, respectively) of **2** to the active site of TACE (shown as surface with zinc colored orange, PDB code: 3LOT). The S1 and S1' subsites are also indicated. (B) Stick representation showing the zinc binding of **2** and hydrogen bonding interactions (dashed lines).

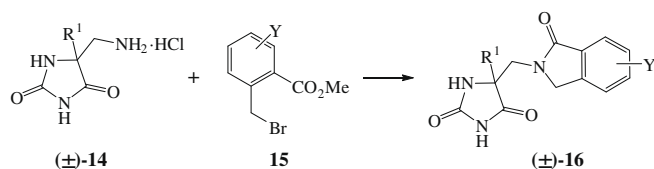


**Scheme 1.** Reagents and conditions: (a)  $\text{Bn}_2\text{NH}$ ,  $\text{Et}_3\text{N}$ , THF, rt, 3 days, 89%; (b) KCN,  $(\text{NH}_4)_2\text{CO}_3$ ,  $\text{EtOH}/\text{H}_2\text{O}$  (1:1), 70 °C 8 h, 86%; (c)  $\text{H}_2$ , 50 psi,  $\text{Pd}(\text{OH})_2/\text{C}$ ,  $\text{EtOH}/\text{MeOH}$  (5:1), rt, 48 h, 95%; (d) 5-methoxy-2-nitrobenzoic acid, EDCl, HOBT, NMM, DMF, rt, 16 h, 85%; (e) Zn, NaOH,  $\text{MeOH}/\text{H}_2\text{O}$  (1:1), 75 °C, 20 h, 14–69%.

zylamine to afford **5** which was converted to a hydantoin via the Bucherer–Bergs reaction. Reductive debenzoylation yielded the desired amine **6**. Compound **6** was coupled with 5-methoxy-2-nitrobenzoic acid to afford amide **7** which was converted to **3** in the presence of zinc and NaOH in low to moderate yield.<sup>13</sup>

Compound **3** has a TACE  $K_i$  of 23 nM and the X-ray structure revealed that **3** bound in the manner expected from modeling (Fig. 3A). The stereochemistry of the hydantoin was determined to be *R*. The corresponding C5 methoxy analog **8** was equipotent to **3**. Increasing steric bulk of the C5 or C6 substituent resulted in a 5–10-fold loss in potency (compounds **9–11**). 5,6-Dimethoxy analog **12** was also less active. Phenyl substitution on the hydantoin (**13**) showed a fourfold improvement of activity compared with **3** (6 nM vs 23 nM).

The length of the hydrogen bond between the indazole NH and the C=O of Pro437 was determined to be 3.2 Å in the X-ray structure (Fig. 3A), suggesting that this may not be a key interaction. This lead us to explore other ring systems (shown in Table 2) as the core structure of the hydantoin TACE inhibitors. Compounds in Table 2 were prepared as described in Scheme 2.<sup>14</sup> Compound



Scheme 2. Reagents and conditions: DIPEA, DMF, rt, 16 h, 54–72%.

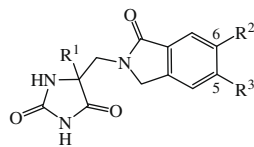
**14** was prepared as described in Scheme 1. Benzyl bromide **15** was prepared by bromination of the corresponding toluene derivatives.<sup>15</sup> The target compounds **16** were obtained in moderate to good yields.

As shown in Table 2, isoindolin-1-one **17** showed excellent activity. It confirmed that the H-bond between the indazole NH and the C=O of Pro437 in **3** is not a key interaction and suggested that a methylene group might fit better in this position. The sulfonamide **18** is a much weaker TACE inhibitor. The hexahydroimidazo[1,5-*a*]pyridin-3(5*H*)-one analog **19** and tetrahydro-1*H*-pyrrolo[1,2-*c*]imidazol-3(2*H*)-one analog **20** are also much weaker than **17**. Pyridyl analogs **21** and **22** are less active whereas **23** showed good activity. In **21**, the pyridyl nitrogen (N7) reaches into a hydrophobic pocket, and in **22**, there is a repulsion between the pyridyl nitrogen (N4) and the carbonyl oxygen of Tyr 436. However, in **23**, the pyridyl nitrogen (N5) forms a hydrogen bond to a conserved water molecule at the bottom of the S1' pocket.

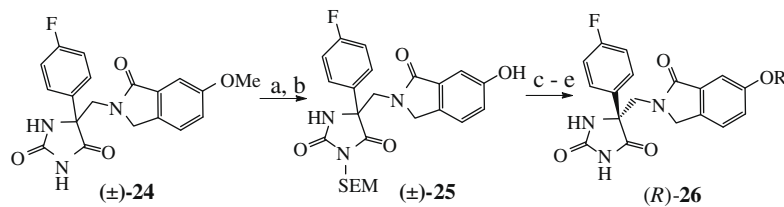
Since isoindolin-1-one analog **17** showed the best TACE activity, additional analogs (shown in Table 3) were prepared. Compounds in Table 3 were prepared based on Schemes 2 or 3. In Scheme 3, compound **24** was demethylated and protected with SEMCl to give **25**. Compound **25** was resolved on a Chiralpak® AD column<sup>16</sup>, and the resulting, desired (*R*)-enantiomer was alkylated with the appropriate alkyl bromides or alkyl iodides. The SEM group was removed to give the final products (*R*)-**26**.

As shown in Table 3, methyl hydantoin analog **27** showed slightly improved activity compared with the 1*H*-indazol-3(2*H*)-one counterparts (Tables 1 and 3). Larger alkyl substituents on the hydantoin moiety led to a loss in potency (e.g., **28**) and this effect was most pronounced with compound **29**. Consistent with

Table 3  
TACE  $K_i$  of isoindolin-1-one analogs



Compound	R <sup>1</sup>	R <sup>2</sup>	R <sup>3</sup>	TACE $K_i$ (nM)
(±)- <b>27</b>	Me	MeO	H	10
( <i>R</i> )- <b>28</b>	Et	MeO	H	56
( <i>R</i> )- <b>29</b>	Benzyl	MeO	H	>500
(±)- <b>30</b>	Ph	MeO	H	3.3
(±)- <b>31</b>	2'-OH-Ph	F	H	9
(±)- <b>32</b>	3'-OH-Ph	Cl	H	10
( <i>R</i> )- <b>33</b>	4'-OH-Ph	MeO	H	1.6
( <i>R</i> )- <b>34</b>	4'-F-Ph	Cl	H	0.4
(±)- <b>35</b>	2',4'-diF-Ph	Cl	H	5.5
( <i>R</i> )- <b>36</b>	4'-F-Ph	MeO	H	0.8
( <i>R</i> )- <b>37</b>	2'-Pyrazinyl	MeO	H	0.7
( <i>R</i> )- <b>38</b>	2'-Furanyl	MeO	H	0.7
( <i>R</i> )- <b>39</b>	1'-Methyl-1 <i>H</i> -pyrazol-4'-yl	MeO	H	1.1
(±)- <b>40</b>	Ph	H	MeO	3.0
( <i>R</i> )- <b>41</b>	4'-F-Ph	H	OH	0.5
(±)- <b>42</b>	4-F-Ph	H	Cl	7.0
( <i>R</i> )- <b>43</b>	4-F-Ph	H		2.4
(±)- <b>44</b>	4-F-Ph	H		9
( <i>R</i> )- <b>45</b>	4-F-Ph	H		332
(±)- <b>46</b>	4-F-Ph	H		1.7



**Scheme 3.** Reagents and conditions: (a) pyridine-HCl, 200 °C, 1 h, 85%; (b) SEMCl, DIPEA, DMF, rt, 5 h, 80%; (c) chiral HPLC separation (see Ref. 16); (d) RI or RBr, Cs<sub>2</sub>CO<sub>3</sub>, DMF, rt, 16 h, 50–95%; (e) HCl, MeOH, 90 °C, 16 h, then TEA, rt, 75–90%.

**Table 4**  
Selectivity data of **3** and **34**

Compound	<b>3</b>	<b>34</b>
TACE K <sub>i</sub> (nM)	28.0	0.43
MMP1 (nM)	3300	176
MMP2 (nM)	4599	1208
MMP3 (nM)	10,000	>40,000
MMP7 (nM)	—	>40,000
MMP9 (nM)	100,000	>40,000
MMP13 (nM)	12,860	>40,000
MMP14 (nM)	31,910	1196
ADAM 9 (nM)	10,000	—
ADAM 10 (nM)	—	245

what we observed in the indazole series, phenyl substitution on the hydantoin (**30**) showed a threefold improvement of activity compared to **27**. Substitution on the phenyl ring is tolerated (**31–36**) and C4' substitution seems to be preferred (**33, 34**). Replacing the phenyl group with heterocycles afforded compounds with similar activities (**37–39**).<sup>17</sup> Both enantiomers of (±)-**40**<sup>16</sup> were prepared. The active isomer (K<sub>i</sub> = 1.7 nM) was determined to be the (R)-isomer by X-ray structure.

As was observed in the 1H-indazol-3(2H)-one series, small substituents on either C5 or C6 offered potent TACE inhibitors (e.g., **34, 36, 40–43**). As the steric bulk of the substituents increases (**44, 45**), a 4–100-fold loss in affinity was observed. However, the bulky quinolinyl analog **46** was tolerated as its binding causes a conformational change of the Ile438-Ser441 loop, to allow the quinolinyl group to be accommodated within the S1'/S3' pockets.<sup>18</sup>

Both the 1H-indazol-3(2H)-one series and isoindolin-1-one series were selective against a group of MMPs as shown by representative compounds **3** and **34** in Table 4. Selected compounds from each series (compounds **13, 34**, and **36**) were also evaluated for their ability to inhibit LPS-induced TNF-α shedding in human whole blood,<sup>19</sup> an indicator of in vivo potency.<sup>20</sup> Relatively weak activities (IC<sub>50</sub>s of 3–16 μM) were observed, suggesting that further improvement is required.

In summary, we have discovered a new series of selective and potent TACE inhibitors using the hydantoin moiety as a zinc-binding ligand. We report the first X-ray structures of inhibitors with a hydantoin zinc ligand bound to TACE. Using structure-based design our initial optimization improved weak micromolar screening hits into sub-nanomolar TACE inhibitors. Further optimization of our lead compounds will be disclosed in future publications.

## References and notes

1. Cerretti, D. P. *Biochem. Soc. Trans.* **1999**, *27*, 219.
2. Vassalli, P. *Annu. Rev. Immunol.* **1992**, *10*, 411.

3. Black, R. A.; Rauch, C. T.; Kozlosky, C. J.; Peschon, J. J.; Slack, J. L.; Wolfson, M. F.; Castner, B. J.; Stocking, K. L.; Reddy, P.; Srinivasan, S.; Nelson, N.; Boiani, N.; Schooley, K. A.; Gerhart, M.; Davis, R.; Fitzner, J. N.; Johnson, R. S.; Paxton, R. J.; March, C. J.; Cerretti, D. P. *Nature* **1997**, *385*, 729.
4. Bemelmans, M. H. A.; van Tits, L. J. H.; Buurman, W. A. *Crit. Rev. Immunol.* **1996**, *16*, 1.
5. Aggarwal, B. B.; Natarajan, K. *Eur. Cytokine Netw.* **1996**, *7*, 93.
6. For a recent review of TACE inhibitors, see: DasGupta, S.; Murumkar, P. R.; Giridhar, R.; Yadav, M. R. *Bioorg. Med. Chem.* **2009**, *17*, 444.
7. (a) Sheppeck, J. E., II; Gilmore, J. L.; Yang, A.; Chen, X.-T.; Xue, C.-B.; Roderick, J.; Liu, R.-Q.; Covington, M. B.; Decicco, C. P.; Duan, J. J.-W. *Bioorg. Med. Chem. Lett.* **2007**, *17*, 1413; (b) Sheppeck, J. E., II; Gilmore, J. L.; Tebben, A.; Xue, C.-B.; Liu, R.-Q.; Decicco, C. P.; Duan, J. J.-W. *Bioorg. Med. Chem. Lett.* **2007**, *17*, 2769; (c) Sheppeck, J. E.; Tebben, A.; Gilmore, J. L.; Yang, A.; Wasserman, Z. R.; Decicco, C. P.; Duan, J. J.-W. *Bioorg. Med. Chem. Lett.* **2007**, *17*, 1408.
8. Rosner, K. E.; Guo, Z.; Orth, P.; Shipp, S.; Shih, N.-Y.; Niu, X.; Lundell, D. J.; Curran, P. J.; Dai, C.; Deng, Y.; Girijavallabhan, V. M.; Hong, L.; Lavey, B. J.; Lee, J. F.; Li, D.; Liu, Z.; Popovici-Muller, J.; Ting, P. C.; Vaccaro, H.; Wang, L.; Wang, T.; Yu, W.; Zhou, G.; Niu, X.; Sun, J.; Kozlowski, J. A.; Lundell, D. J.; Madison, V.; McKittrick, B.; Piwinski, J. J.; Shih, N.-Y.; Siddiqui, M. A.; Strickland, C. O. *Bioorg. Med. Chem. Lett.* **2010**, *20*, 1189.
9. Guo, Z.; Orth, P.; Wong, S.-C.; Lavey, B. J.; Shih, N.-Y.; Niu, X.; Lundell, D. J.; Madison, V.; Kozlowski, J. A. *Bioorg. Med. Chem. Lett.* **2009**, *19*, 54.
10. Ingram, R. N.; Orth, P.; Strickland, C. L.; Le, H. V.; Madison, V.; Beyer, B. M. *Protein Eng., Des. Selection* **2006**, *19*, 155.
11. Maskos, K.; Fernandez-Catalan, C.; Huber, R.; Bourenkov, G. P.; Bartunik, H.; Ellestad, G. A.; Reddy, P.; Wolfson, M. F.; Rauch, C. T.; Castner, B. J.; Davis, R.; Clarke, H. R. G.; Petersen, M.; Fitzner, J. N.; Cerretti, D. P.; March, C. J.; Paxton, R. J.; Black, R. A.; Bode, W. *Proc. Natl. Acad. Sci. U.S.A.* **1998**, *95*, 3408.
12. Cross, J. B.; Duca, J. S.; Kaminski, J. J.; Madison, V. S. *J. Am. Chem. Soc.* **2002**, *124*, 11004.
13. Bruneau, P.; Delvare, C.; Edwards, M. P.; McMillan, R. M. *J. Med. Chem.* **1991**, *34*, 1028.
14. Compounds **19** and **20** were made by treating amine **6** with *tert*-butyl 2-formylpyrrolidine-1-carboxylate or 2-formylpiperidine-1-carboxylic acid *tert*-butyl ester with titanium isopropoxide and NaBH<sub>3</sub>CN followed by deprotection of the Boc protecting group. The resulting material was then subjected to carbonyl diimidazole in the presence of Hünig's base to give **19** and **20**, respectively.
15. For the synthesis method of methyl 2-(bromomethyl)-5-methoxybenzoate, please see patent: Yu, W. et al. WO 2007084415, 2007.
16. For chiral HPLC separation conditions, see Ref. 15.
17. For the synthesis of the corresponding 2-amino-1-heteroaryl-ethanone, (a) from heteroaryl halide, see Chen, Z. et al. WO 2005056562, 2005.; from 2-bromo-1-heteroaryl-ethanone, see: (b) Loughlin, W. A.; Henderson, L. C.; Elson, K. E.; Murphy, M. E. *Synthesis* **2006**, 1975.
18. This is based on a X-ray crystal structure of the corresponding R<sup>1</sup> = phenyl compound within the active site of the TACE enzyme and additional X-ray data on compounds within the hydantoin series that we have not discussed in detail due to space limitations. The shift of this loop is very similar to that previously described in Niu, X.; Umland, S.; Ingram, R.; Beyer, B. M.; Liu, Y.-H.; Sun, J.; Lundell, D.; Orth, P. *Arch. Biochem. Biophys.* **2006**, *451*, 43.
19. Human whole blood is diluted 1:1 with serum free medium (RPMI, L-glutamine, Pen-Strep, HEPES) and incubated with a compound in a final volume of 360 μL for 1 h at 37 °C. Forty microliters of LPS (10 g/mL) is then added. Supernatant is collected after 3.5 h incubation and the concentration of TNF-α is determined by ELISA (R&D Systems).
20. Please see the following reference for a discussion of the correlation of whole blood activity with in vivo efficacy: Qian, M.; Bai, S. A.; Brogdon, B.; Wu, J.-T.; Liu, R.-Q.; Covington, M. B.; Vaddi, K.; Newton, R. C.; Fossler, M. J.; Garner, C. E.; Deng, Y.; Maduskuie, T.; Trzaskos, J.; Duan, J. J.-W.; Decicco, C. P.; Christ, D. *Drug Metab. Dispos.* **2007**, *35*, 1916.